Experimental and numerical comparison of the wave dynamics and guy wire forces of a very light FOWT considering hydroelastic behavior

Conference Paper · November 2018

CITATIONS
0

READS
26

8 authors, including:

Lucas Henrique Souza do Carmo
University of São Paulo
3 PUBLICATIONS **0** CITATIONS
SEE PROFILE

Daniel Prata Vieira
University of São Paulo
17 PUBLICATIONS **11** CITATIONS
SEE PROFILE

Pedro Cardozo de Mello
University of São Paulo
28 PUBLICATIONS **32** CITATIONS
SEE PROFILE

Edgard Malta
University of São Paulo
20 PUBLICATIONS **55** CITATIONS
SEE PROFILE

Proceedings of the ASME 2018 1st International Offshore Wind Technical Conference
IOWTC2018
November 4-7, 2018, San Francisco, CA

IOWTC2018-1057

EXPERIMENTAL AND NUMERICAL COMPARISON OF THE WAVE DYNAMICS AND GUY WIRE FORCES OF A VERY LIGHT FOWT CONSIDERING HYDROELASTIC BEHAVIOR

Jiang Xiong
Dept. of Ocean Tech., Policy and Environ.
University of Tokyo
Tokyo, Japan

Lucas H. S. do Carmo
Dept. of Naval Arch. & Ocean Eng.
University of São Paulo
São Paulo, Brazil

Daniel P. Vieira*
Technomar
Engenharia Oceânica
São Paulo, Brazil

Pedro C. de Mello
Dept. of Naval Arch. & Ocean Eng.
University of São Paulo
São Paulo, Brazil

Edgard B. Malta
Technomar
Engenharia Oceânica
São Paulo, Brazil

Alexandre N. Simos
Dept. of Naval Arch. & Ocean Eng.
University of São Paulo
São Paulo, Brazil

Hideyuki Suzuki
Dept. of Systems Innovation
University of Tokyo
Tokyo, Japan

Rodolfo T. Gonçalves
Dept. of Systems Innovation
University of Tokyo
Tokyo, Japan

ABSTRACT

Floating offshore wind turbines (FOWT) have many pros and cons. Among the pros, we can mention the availability of more constant winds and a velocity more suitable to the use of turbines in their optimum efficiency. Among the cons, there are the high costs for installation, mooring lines and the large length of cables required for the energy transmission. In this context, saving structural weights of the floater is, certainly, very welcome.

This paper describes the results of an experimental campaign of a 1/80th scale model FOWT performed in a wave basin. The model consists of a central column connected by pontoons to three equally spaced columns by an angle of 120 degrees. The offset columns are connected to the central tower by guywires. Being structurally light, both pontoons and guywires are subject to the effects of hydroelasticity. In these preliminary tests of the concept, only waves were considered, hence wind effects are not yet addressed. The analysis is based on the first order motions of the FOWT, the tension at the guywires, and the strain at the pontoons.

The results are compared with numerical simulations obtained with the software NK-UTWind, developed at the University of Tokyo, and METiS - USP, currently being developed at the University of São Paulo. Furthermore, the floater motions are also analyzed using the commercial software WAMIT, to provide a better insight on the physics involved by using a different approach to the calculation of hydrodynamic forces.

1 INTRODUCTION

Considering the growing scenario for wind farms, both onshore and offshore, the study of new concepts is essential to develop and expand the use of wind in a greater proportion of the

*Address all correspondence to this author.
dprata@technomar.com.br

world energy matrix. The possibility of bringing these systems to the deep seas at distances farther from shore allows the use of more constant winds. However, this considerably increases installation, mooring lines and transmission cables costs.

Lighter, easier to build and to install structures are essential to minimize costs. The concept, presented in Figure 2, consists in an arrangement with a central tower connected by pontoons to three equally spaced columns by an angle of 120 degrees. The columns are connected to the central tower by wires used to reinforce the structure of the floating unit, allowing it to be lighter. Thus, being structurally light, both pontoons and guy wires are subject to the effects of hydroelasticity, requiring the evaluation of the forces and deformations due to the waves on the various structural elements.

In [1] a comprehensive literature survey of the advances in floating wind turbines is presented. In this work the several concepts were listed and categorized. According to this work, the concept presented here is named as a semi-submersible type (column stabilized) floating wind turbine.

The use of floating structures to support wind turbines, despite being a promising idea, still needs further studies and development, requiring a broader database to prove the effectiveness of its use. In this sense, the work of [2] presents a recent review of the scaled model tests carried out so far. Another examples for model tests are the work of [3], [4] and [5]. From the numerical point of view it is possible to mention the works of [6] and [7].

The text is divided in three sections: Methodology, Results and Conclusions. In the Methodology section, the configurations adopted for the experimental approach, model layout, mooring lines, calibration and validation of hydrostatic and hydrodynamic parameters are presented. It is worth mentioning that, as a first approach, only wave forces were considered in the analysis. Then, the two numerical approaches are introduced: NK-UTWind of the University of Tokyo and METiS-USP of the University of São Paulo, besides the commercial software WAMIT. In the Results section we present the main comparisons between the parameters measured in the tests and the results obtained with the numerical simulations. These results include the motions of the vessel and the deformations measured in the guy wires and in the pontoons. Finally the general conclusion are listed.

2 METHODOLOGY

2.1 Experimental Setup

The experimental model tests were conducted in the Hydrodynamic Calibrator of the University of São Paulo (CH-TPN), shown in Figure 1. The wave basin is a squared 14m x 14m x 4m (length, width, depth) form, equipped with 148 active-absorber wave generators. The equipment can generate the incident waves and absorb diffracted and radiated waves by the model, following specific control algorithms, as discussed by [8]. The waves peak period range is about 0.8s up to 2.5s in model scale. To achieve the intended peak periods the model tests were made in scale 1/80th.

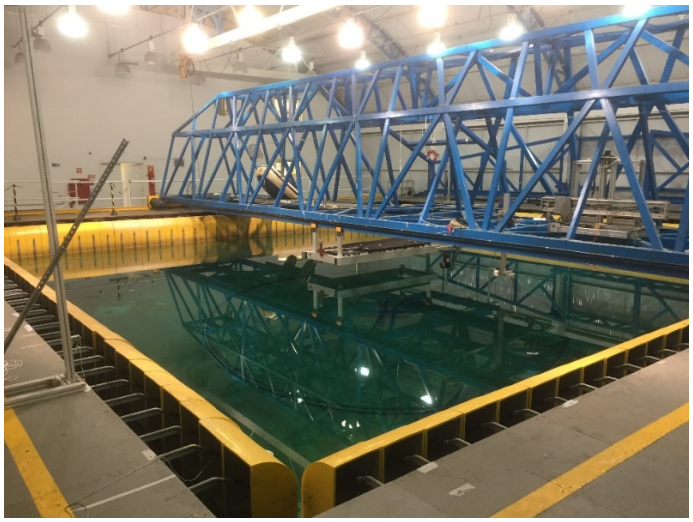

FIGURE 1: University of São Paulo Wave Basin

The model was constructed to represent the geometry, flexural rigidity of the vertical tower and pontoon, hydrostatic and hydrodynamic behavior of FOWT prototype. Table 1 presents the geometry of the modeled FOWT. Table 2 shows the main hydrostatic, dynamic and structural characteristics of the system. Due to the model symmetry, the natural periods in roll and pitch are the same. The guy-wires were made by stained steel cables with non-scaled stiffness. In order to model the pontoons and tower, the core beam was designed to match the scaled flexural rigidity (EI) of the prototype. The pontoon buoyancy and geometry are obtained by segmented blocks of urethane foam covering the steel core beam; six blocks per pontoon. The hydrostatic characteristic were verified with free decay tests, while the flexural rigidities of the tower and pontoons were calculated based on the geometry and material of the core beams.

The connection between the tower and the pontoons had a stiff joint. The four columns are modeled by cylinders made of fiberglass and urethane. The lower part of each side column had a ballast to calibrate the vertical center of gravity and inertia. Figures 2 and 3 present the model overview with the characteristics described above. The CoG of the model defined the model CoC system; X axis along one of the pontoons with the Z axis upwards. The guy-wires connect the junctions between columns and pontoons to the top of the tower. Pretensioning was imposed on the wires so that they do not unbend during the tests.

The model motions were measured by Qualisys optical tracking system. To provide accuracy and redundancy for motion measurement, 4 tracking cameras with 5 passive markers on

TABLE 1: Prototype and experimental model main dimensions

	Dimension	Prototype	Exp. Model (1/80)
Tower	Diameter	7 *m*	87.5 *mm*
	Height	105 *m*	1312.5 *mm*
Columns	Diameter	7 *m*	87.5 *mm*
	Height	25 *m*	312.5 *mm*
Pontoons	Length	30 *m*	375 *mm*
	Height	5 *m*	62.5 *mm*
	Width	7 *m*	87.5 *mm*

TABLE 2: Principal Design of Prototype and Experiment Model

Item	Prototype	Exp. Model(1/80)
Displacement	5774 *ton*	11.25 *kg*
KB	4.59 *m*	57.48 *mm*
BM	16.08 *m*	201.46 *mm*
KG	8.31 *m*	104.64 *mm*
GM	12.36 *m*	154.30 *mm*
T_n Heave	16.6 *s*	1.86 *s*
T_n Roll/Pitch	20.6 *s*	2.28 *s*
EI Pontoon	$2.707 \cdot 10^{11}\ Pa \cdot m^4$	$8.26 \cdot 10^{1}\ Pa \cdot m^4$
EI Tower	$5.031 \cdot 10^{11}\ Pa \cdot m^4$	$1.54 \cdot 10^{2}\ Pa \cdot m^4$

the base of the tower were used. Because of the redundancy of cameras to track each marker, the marker position error is always less than 1.0 mm. In the same way, with 5 markers on the platform, the measurement of six degree of freedom movement (surge, sway, heave, roll, pitch and yaw) is always redundant, since 3 markers are enough to measure the motions. The sample frequency adopted in the model scale movement measurement is 100 Hz.

To measure the bending of the pontoon cores and of the tower core, strain gauges were attached in selected points of interest, as illustrated by Figure 4. Markers FP denote pontoons points that are 135mm and 272mm in radial distance to the center of the model. Markers FC denote points at the center tower core that are aligned to each pontoon, 100mm above the model bottom. These gauges were calibrated in strain (μS). The markers

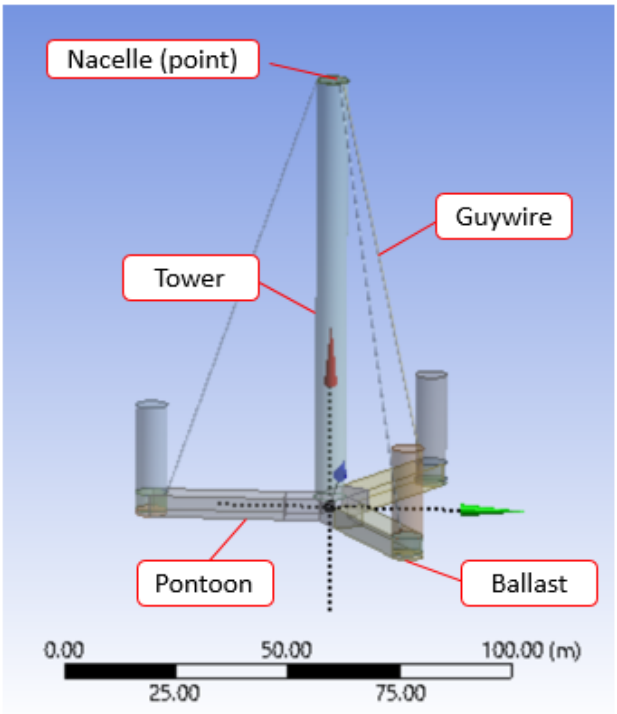

FIGURE 2: Prototype overview

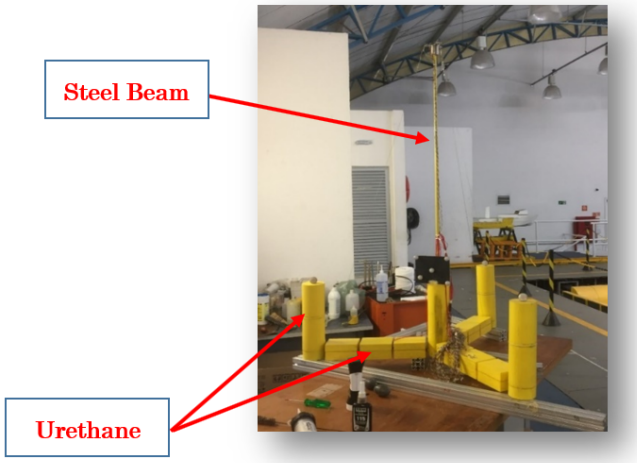

FIGURE 3: Experimental model overview

FG denote guy-wire tension, and these gauges were calibrated in Newtons (N).

The wave incidences in the experiments were 180 deg (head), 195 deg, 210 deg, 225 deg and 240 deg. Since the angle between pontoons/side columns is 120 deg, a heading sweep of 60 deg covers all wave incidences of the model. To provide

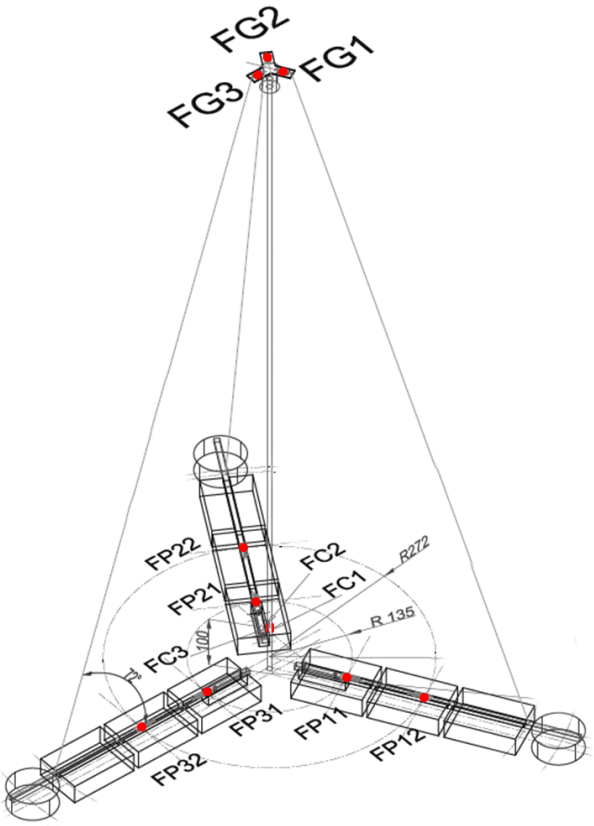

FIGURE 4: Strain gauges locations

corresponding headings, three horizontal anchoring lines were used. The connection points were located in each of the offset columns. In the end of each line there is a spring connected to the borders of the wave basin. The spring stiffness is 2.2 N/m and pretension is 0.49 N, corresponding, in full scale, to 14 kN/m and 252 kN.

Figure 5 presents the wave basin arrangement for the experiments. A set of markers on the wave basin borders denotes the connection lines positions for each heading. A set of three wave probes measured the waves during the experiments, while an additional wave probe was used at the model position for wave calibration. On bridge carriage, four optical tracking cameras measured the model movement.

A set of four types of waves was defined for the experiments. Transient and white noise waves provide a rapid RAO evaluation. It was made covering all range of periods of interest using low wave elevation in linear condition. Table 5 shows the white noise wave characteristics. Three irregular waves, modeled by JONSWAP parametric spectrum, were defined to study the model behavior in typical seas. These waves were made for all headings, and their characteristics are given in Table 3. In headings of 180 deg, 210 deg and 240 deg, a set of regular waves

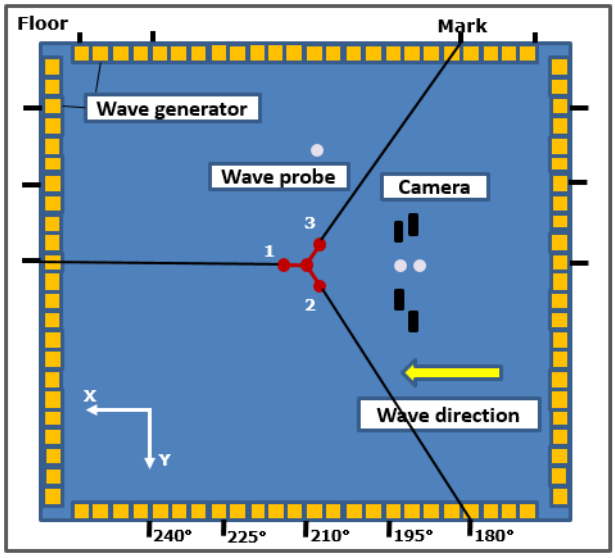

FIGURE 5: Top-View of the Ocean Basin and Coordinate System

was made to study the damping in the heave natural period and to cover a range of periods of operational cases, as presented in Table 4.

2.2 Numerical models

Besides the experimental tests, the full scale FOWT was analyzed using three different software with different objectives:

1. NK-UTWind, a software for the coupled analysis of floating offshore wind turbines, developed by ClassNK and the University of Tokyo. The objective is to compare the first order motions of the floater, the tension at the guy-wires, and the strain at selected positions on the pontoons calculated by NK-UTWind with the ones provided by the experiment, aiming at validating the code for analyzing different FOWT concepts derived directly from the one studied in the experimental campaign;

2. METiS-USP, an in-house code for the analysis of floating systems with little diffraction, such as floating offshore wind turbines, currently under development at the University of São Paulo. Since it is still in an early phase of development, the first order motions calculated by the other software and the ones measured in the experiment are an important way of validating the code. Both NK-UTWind and METiS-USP employ Morison's equation for calculating the hydrodynamic loads, as explained below;

3. WAMIT, a commercial Boundary Element Method code for analyzing wave interactions with offshore structures, which evaluates the hydrodynamic loads through the solution of

TABLE 3: Irregular wave characteristics

WAVE ID	TYPE	Wave Characteristics (Prototype)			Wave Characteristics (Model)		
		H_s (m)	T_p (s)	Duration (h)	H_s (mm)	T_p (s)	Duration (s)
FOWT-IRR01	JONSWAP	2.5	9.0	3.0	31.6	1.006	1207
FOWT-IRR02	JONSWAP	9.8	13.5	3.0	122.5	1.509	1207
FOWT-IRR03	JONSWAP	4.0	16.1	3.0	50.6	1.800	1207

TABLE 4: Regular wave characteristics

WAVE ID	Prototype		Model	
	T_p (s)	H_s (m)	T_p (s)	H_s (mm)
FOWT-REG01	16.350	0.5	1.83	6.25
FOWT-REG02	16.350	1.0	1.83	12.5
FOWT-REG03	16.350	2.0	1.83	25
FOWT-REG04	16.350	4.0	1.83	50
FOWT-REG05	16.350	5.0	1.83	62.5
FOWT-REG06	16.350	6.0	1.83	75
FOWT-REG07	6.000	3.0	0.67	37.5
FOWT-REG08	7.000	3.0	0.78	37.5
FOWT-REG09	8.000	3.0	0.89	37.5
FOWT-REG10	9.000	3.0	1.00	37.5
FOWT-REG11	10.000	3.0	1.12	37.5
FOWT-REG12	11.000	3.0	1.23	37.5
FOWT-REG13	12.000	3.0	1.34	37.5
FOWT-REG14	13.000	3.0	1.45	37.5
FOWT-REG15	14.000	3.0	1.57	37.5
FOWT-REG16	15.000	3.0	1.68	37.5
FOWT-REG17	16.000	3.0	1.79	37.5
FOWT-REG18	17.000	3.0	1.90	37.5

the radiation/diffraction problem in frequency domain. As it is based in a different hydrodynamic method than both NK-UTWind and METiS-USP, simulations with WAMIT are useful to highlight the conditions in which each method is better at reproducing the experimental results.

Details about how the FOWT is modeled in each of the software are provided below, as well as a brief explanation of the part of the theory behind NK-UTWind and METiS-USP that is the most relevant for this work.

2.2.1 WAMIT

The WAMIT simulation was conducted with a higher order mesh composed of 30 patches. In this method, the geometry of the body is described by B-splines and all quantities are continuous inside each patch (details can be found in [9]). After a convergence analysis, the panel size parameter was set to 4. An illustration of the mesh is given in Figure 6.

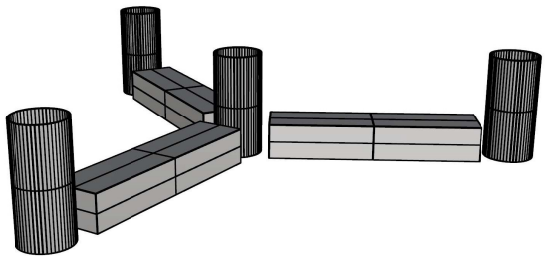

FIGURE 6: Higher order mesh used in the WAMIT simulation.

Since WAMIT is a potential theory code, it is necessary to include additional damping terms to (partially) account for viscous damping, especially for the motions in the vertical directions (heave, roll and pitch), in order to avoid spurious amplifications around the resonance frequency of each degree of freedom. Based on results from previous works and on the author's experience, an additional damping of 5% of the critical damping is a good estimation (see, for example, [10] for a discussion on the damping coefficient of semi-submersible FOWT).

TABLE 5: White noise wave characteristics

WAVE ID	Wave Characteristics (Prototype)				Wave Characteristics (Model)			
	T_p^{min} (s)	T_p^{max} (s)	H_s (m)	Duration (h)	T_p^{min} (s)	T_p^{max} (s)	H_s (mm)	Duration (s)
FOWT-WHI01	6.6	17.9	2	0.50	0.74	2.00	25.00	200

2.2.2 METiS-USP

As stated above, METiS-USP is an in-house code under development at the University of São Paulo for the time domain analysis of floating systems with little diffraction. The structure is considered as a rigid body comprised of slender circular and rectangular cylinders, in such a way that the application of Morison's equation for the calculation of hydrodynamic forces yields good results. Besides, as cylinders are very simple geometric shapes, the calculation of the displaced volume and of the center of volume is very straightforward, meaning that the hydrostatic force can be easily calculated at each time step.

Adopting a local coordinate system $Oxyz$ for each cylinder, with the origin O at the base of the cylinder, z the axial direction, and x and y the two axes of symmetry of a rectangular cylinder (or two arbitrary axes for a circular cylinder), the forces acting at each section are given by:

$$\begin{aligned}\begin{bmatrix} dF_x \\ dF_y \end{bmatrix} =& \rho A \begin{bmatrix} (1+C_{ax})\,\dot{u}_x \\ (1+C_{ay})\,\dot{u}_y \end{bmatrix} - \rho A \begin{bmatrix} C_{ax}\,\ddot{q}_x \\ C_{ay}\,\ddot{q}_y \end{bmatrix} \\ &+ \frac{1}{2}\rho |\vec{u}_p - \vec{q}_p| \begin{bmatrix} D_y\, C_{Dx}\,(u_x - \dot{q}_x) \\ D_x\, C_{Dy}\,(u_x - \dot{q}_y) \end{bmatrix}\end{aligned} \tag{1}$$

where ρ is the fluid density, A is the cross sectional area, $\vec{u}_p = u_x\vec{e}_x + u_y\vec{e}_y$ is the component of the fluid velocity that is perpendicular to the cylinder axis, and $\vec{q}_p = q_x\vec{e}_x + q_y\vec{e}_y$ is the component of the cylinder displacement, calculated at that specific section, that is perpendicular to the cylinder. D_x and D_y are the width (or diameter) of the cylinder, C_{ax} and Cay the added mass coefficients in x and y direction, and C_{Dx} and C_{Dy} the drag coefficients in x and y direction. The total force acting at each cylinder is obtained by integrating the infinitesimal forces calculated at a certain number of nodes along its length using Simpson's rule. The nodes position of each cylinder is updated at each time step for the evaluation of the hydrodynamic loads.

In the axial direction, the force is calculated using the following equation:

$$\begin{aligned}F_z =& \frac{1}{2}\rho\, C_{Dz} A |u_z - \dot{q}_z|(u_z - \dot{q}_z) \\ &+ \rho\, C_{az} V_R\,(\dot{u}_z - \ddot{q}_z) + p_b S_b - p_t S_t\end{aligned} \tag{2}$$

with $V_R = \frac{4}{3}\pi\left(\frac{D_x+D_y}{2}\right)^3$; p_b and p_t the dynamic pressure, due only to the undisturbed incoming wave, at the bottom and at the top of the column; and S_b and S_t the surface of the bottom and top faces of the column. The term $p_t S_t$ is non-zero only when the column is submerged, such as when modeling heave plates.

For the FOWT studied in this work, the drag and added mass coefficients of the pontoons were determined from the results presented [11], while the drag coefficient of the columns was calculated with the results from [12]. As both the drag and added mass coefficients depend on the Keulegan-Carpenter and Reynolds number, an average value was taken for all the wave conditions, and care was taken to keep the resulting added mass in surge and heave close to the ones obtained with WAMIT. For the added mass coefficient of the columns, the value calculated from potential theory was adopted. The axial drag coefficient of both the pontoons and the columns was considered to be zero, as it must be negligible face the drag due to the other elements. The resulting coefficients are provided in Table 6. For the pontoons, x is the horizontal direction and y is the vertical.

TABLE 6: Added mass and drag coefficients adopted in METiS-USP

Coefficient	Columns	Pontoons
C_{Dx}	0.7	4.0
C_{Dy}	0.7	5.0
C_{Dz}	0.0	0.0
C_{ax}	1.00	0.65
C_{ay}	1.00	1.20
C_{az}	0.80	0.00

For calculating the fluid velocity, the waves are modeled following linear theory (Airy wave) with no stretching. For now, the restoration due to the mooring system is modeled as a linear

stiffness matrix. The aerodynamic loads on the blades is under development.

2.2.3 NK-UTWind

NK-UTWind is a software for the coupled analysis of floating offshore wind turbines. In a complete FOWT modeling, the blades and the floater are modeled as frame structures with beam elements. The mooring lines are described according to lumped mass model, while the aerodynamic load on the blades is computed using Blade Element Momentum Theory. A complete description of the theory implemented in NK-UTWind can be found in [13]. For the present work, the most relevant part of NK-UTWind theory is the calculation of the hydrodynamic load.

As most FOWTs are comprised of slender structural elements, such as cylinders, NK-UTWind employs Morison elements for the evaluation of hydrostatic restoration and hydrodynamic loading (see Eq. 1). The restoring force is computed at each time step by summing the hydrostatic pressure on each element at the instantaneous displaced position, while the hydrodynamic force is calculated using Morison's equation. Wheeler's strech method is used to estimate the wave velocity field, and the instantaneous wave load is evaluated considering submergence of each structural element.

The coefficients added mass and drag coefficients adopted in NK-UTWind simulation are given in Table 7. It is important to mention that although similar, there is one key difference between the hydrodynamic model in NK-UTWind and METiS-USP. In NK-UTWind, Morison elements are modeled as ellipses, so it is necessary to convert the coefficients of a rectangular cylinder to those of a elliptic cylinder, making sure that the sectional area, added mass and drag force remain the same.

TABLE 7: Added mass and drag coefficients adopted in NK-UTWind

Coefficient	Columns	Pontoons
C_{Dx}	1.0	1.0
C_{Dy}	1.0	1.0
C_{Dz}	0.0	0.0
C_{ax}	1.00	1.00
C_{ay}	1.00	1.00
C_{az}	0.80	0.80

3 RESULTS

The main results obtained during the experimental campaign were the first order motions, the tension at the guy-wires, the tower bottom strain, and the strain at selected positions on the pontoons. The motion RAOs are useful for validating the software and indicating the wave conditions in which they are reliable, while the hydroelastic results bring interesting conclusions by themselves, besides providing a means of validating NK-UTWind for the calculation of stress at the guy-wires.

3.1 Motion RAOs

Figures 7 to 10 present the motion RAOs (Response Amplitude Operators) measured in the experiment and the ones calculated with the three different software for a wave direction of 210°. From the experimental campaign, only the results for the regular waves (Table 4) and for the white-noise wave (Table 5) are shown, as the other waves yielded similar RAOs. The wave direction of 210°was chosen to illustrate the response of the floater, since all the degrees of freedom show significant motion. Besides, the conclusions are the same that can be drawn from the other wave directions. Finally, given the symmetry of the floater, the overall behavior in surge/sway and in roll/pitch is the same (not for the same wave direction, of course). Hence, only the RAOs of surge, heave, pitch and yaw are presented.

In surge (or sway), both WAMIT and NK-UTWind agree very well with the experimental results. METiS-USP, however, shows a significant difference for longer wave periods, with the maximum relative error equal to approximately 24% when the wave direction is 180°.

For the heave motion, all the results show a good adherence in general. The main exception is around 15.6 s, where WAMIT is not able to reproduce the experimental result, which was already expected due to the motion being caused by viscous effects. Moreover, NK-UTWind underestimates the motion for wave periods between 12 s and 17 s.

In pitch (or roll), NK-UTWind and METiS-USP agree well between each other for short waves, and they both underestimate the motion measure in the experiments. This may be due to diffraction effects, which become more relevant as the wave gets shorter. Although large in relative terms (the worst case is around 70% for $T = 11$ s, when NK-UTWind and METiS predict a nearly null motion), they are small in absolute terms, as the maximum difference is around 0.13° for $T = 7$ s. For longer waves, METiS-USP agrees well with the experiment, while UTWind provides larger amplitudes.

Finally, all the results in yaw are very similar, with no significant aspect worth mentioning.

3.2 Tension at structures

Due to the cancellation of the pitch motion (around 12 s), which coincides with a wavelength approximately twice the out-

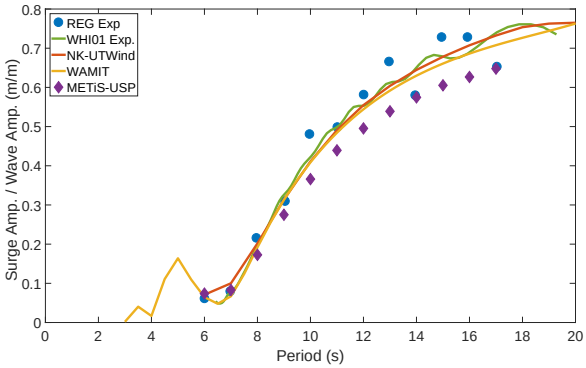

FIGURE 7: Surge motion comparison between the experiment and numerical simulations for a wave direction equal to 210°

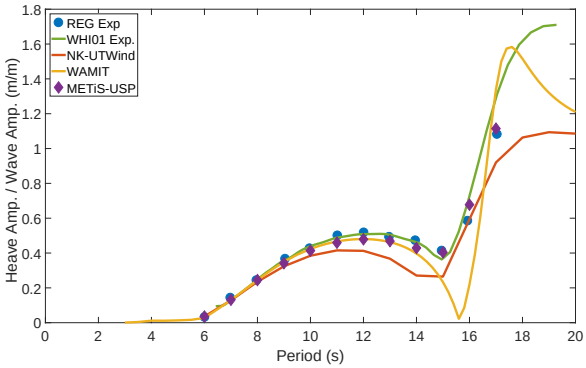

FIGURE 8: Heave motion comparison between the experiment and numerical simulations for a wave direction equal to 210°

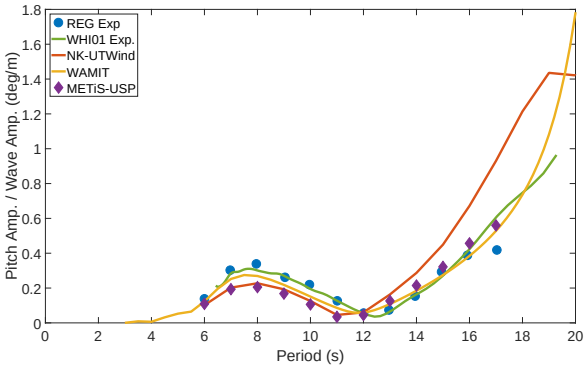

FIGURE 9: Pitch motion comparison between the experiment and numerical simulations for a wave direction equal to 210°

side diameter of the platform, the acceleration in RNA reduces and the flexural stress in the central column also reduces. Likewise, the strength in the guywires also reduce. In pontoons the force remains constant. In the natural heave period all the twelve sensors measure a large force due to the large heave movement

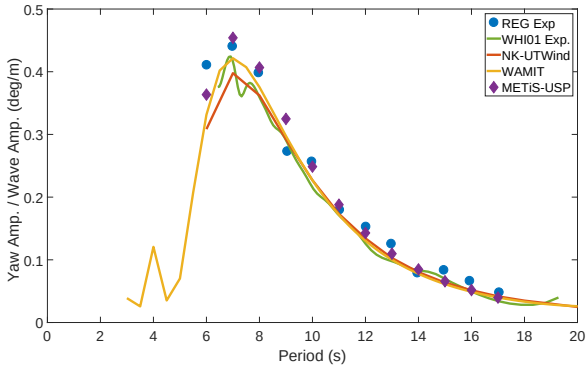

FIGURE 10: Yaw motion comparison between the experiment and numerical simulations for a wave direction equal to 210°

A force peak occurs in all tests on all twelve sensors near 6.6 s. This is the period for which the wavelength is equal to the distance between columns projected in the wave direction. In this condition, the hydrostatic restoration is maximum and causes a large shear force on the hull. It is equivalent to say that in this situation two wave peaks are passing through the outer columns while the central column is near the wave trough.

In a nutshell, there are 3 observed effects:

1. Amplification of all forces in the natural heave period;
2. Cancellation at the wave period that corresponds to the minimum combination of pitch and heave motions, related to a wavelength close to twice the platform diameter;
3. Amplification of the forces when the wavelength is equal to the diameter of the platform.

4 CONCLUSION

This work presented the results of an experimental campaign of the floater of a very-light semi-submersible FOWT. The floater consists of a central column, which sustains the tower, connected by pontoons to three offset columns. The tower is connected by guy-wires to the offset columns. The main results were the first order motions, the tension at the guy-wires, the tower bottom strain, and the strain at selected positions on the pontoons. The motion RAOs were compared with the ones calculated by three different software: NK-UTWind, METiS-USP and WAMIT; while the measured tension at the guy-wires was compared with NK-UTWind only.

The measure motions were useful mainly for validating the software, besides shedding light on some aspectes of the hydroelastic behavior of the floater. The motions obtained showed

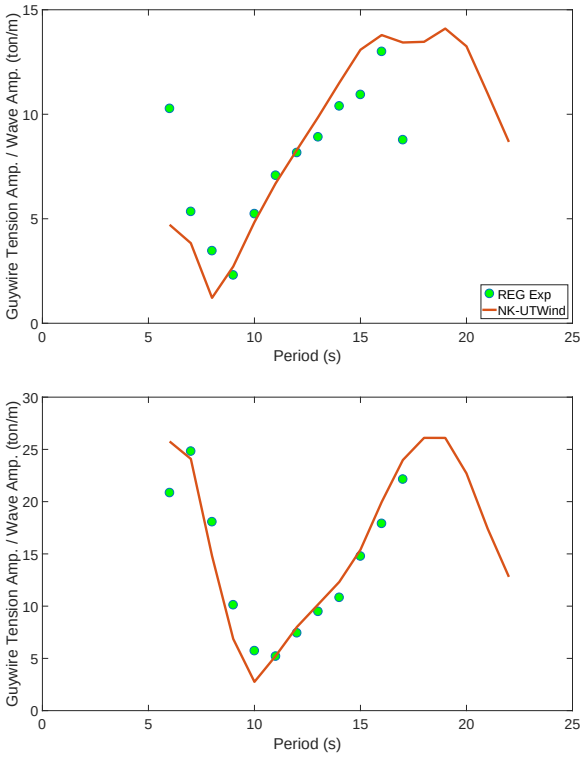

FIGURE 11: Tension at guy-wires number 1 (top) and 3 (bottom) obtained in the experiment and calculated with NK-UTWind for a wave direction of 240°

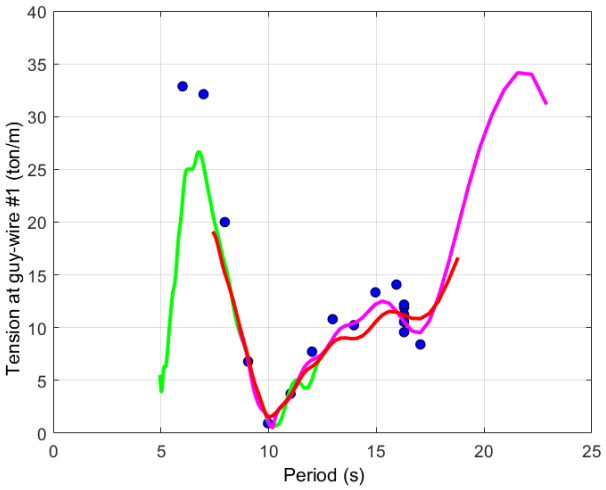

FIGURE 12: Tension at guy-wires number 1 for a wave direction of 180°. The blue marks correspond to the regular waves, while the green, red and magenta lines correspond to the irregular waves IRR01, IRR02 and IRR03, respectively.

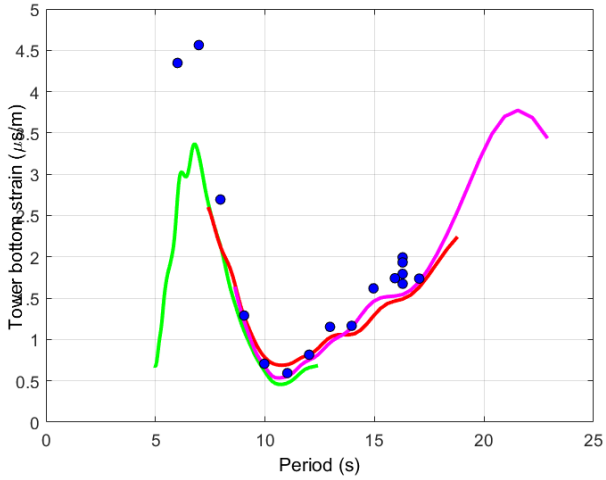

FIGURE 13: Tower bottom strain for a wave direction of 180°. The blue marks correspond to the regular waves, while the green, red and magenta lines correspond to the irregular waves IRR01, IRR02 and IRR03, respectively.

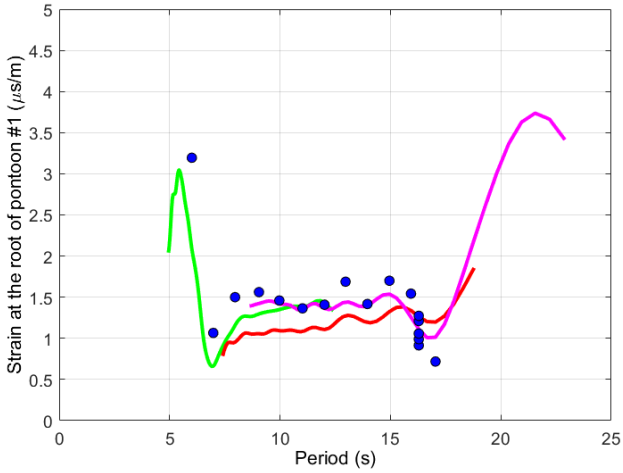

FIGURE 14: Strain at the root of the pontoon number 1 for a wave direction of 180°. The blue marks correspond to the regular waves, while the green, red and magenta lines correspond to the irregular waves IRR01, IRR02 and IRR03, respectively.

a good general agreement. In surge/sway WAMIT and NK-UTWind agreed well with the experimental results, while METiS showed reasonable differences for larger wave periods. For the heave motions, all the results adhered very well, except for the region around 15 s, in which WAMIT could not recover the experimental results, since the movement is due to viscous effects. Besides, NK-UTWind underestimates the heave motion for wave

periods between 12 s and 17 s, and it underestimates the amplitude near the resonant peak, probably due to the calibration of the drag coefficient.

For the pitch/roll motions, both NK-UTWind and METiS-USP agree well between each other, both slightly underpredicting the motion. This may be due to diffraction effects, which become more relevant as the wave gets shorter. Although large in relative terms (the worst case is around 70% for $T = 11$ s, when NK-UTWind and METiS predict a nearly null motion, which doesn't appear in the experiment), they are small in absolute terms, with a maximum difference around 0.13°. For longer waves, METiS-USP agrees well with the experiment, while NK-UTWind provides larger amplitudes.

About the hydroelastic results, it is worth mentioning that the deformation of the guy-wires is a combination of the deformation of the tower and the pontoons. Since both the tower and the pontoons are greatly affected by the pitch motion, it is possible to say that the tension variation at the guy-wires is also dominated by pitch. Hence, the cancellation of the pitch motion around 12 s (which corresponds to a wavelength of approximately twice the outside diameter of the platform) reduces the acceleration of the RNA, leading to a corresponding reduction on the tower bottom strain and on the tension at the guy-wires. In the pontoons, the stress remains constant for a large range of wave periods.

At the heave natural period, all the twelve sensor measured large efforts, due to the large heave motion. Besides, all the sensors measured a force peak at a wave period around 6.6 s, and this behavior was observed in all the tests. This period corresponds to a wavelength equal to the distance between columns projected in the wave direction, meaning that the floater is sagging/hogging, causing large loads on the hull. To summarize, three main hydroelastic effects were observed:

1. Amplification of all forces in the natural heave period;
2. Minimum loads at the wave period for which the combined heave and pitch motions are minimum, which is observed for a wavelength around twice the platform diameter. In this condition, the tension at the guy-wires may be zero, depending on the wave incidence;
3. Amplification of the forces when the wavelength is equal to the diameter of the platform.

Finally, the tension at the guy-wires obtained with NK-UTWind was very close to the ones measure in the experiments, validating the software for this kind of calculation.

ACKNOWLEDGMENT

The authors would like to thank the technical team of the Numerical Offshore Tank - USP for their help during the model tests. Jiang Xiong would like to acknowledge The Japan Society of Naval Architects and Ocean Engineers (JASNAOE) for the financial support of his internship period in Brazil when the model was tested. Lucas Henrique Souza do Carmo acknowledges CAPES, the Brazilian Federal Agency for Post-Graduate Education, for his PhD grant. Alexandre Simos acknowledges CNPq, the Brazilian National Council for Scientific and Technological Development, for his research grant.

REFERENCES

[1] Wang, C., Utsunomiya, T., Wee, S., and Choo, Y., 2010. "Research on floating wind turbines: a literature survey". *The IES Journal Part A: Civil & Structural Engineering,* ***3***(4), pp. 267–277.

[2] Stewart, G., and Muskulus, M., 2016. "A review and comparison of floating offshore wind turbine model experiments". *Energy Procedia,* ***94***, pp. 227–231.

[3] Shin, H., Dam, P. T., Jung, K. J., Song, J., Rim, C., and Chung, T., 2013. "Model test of new floating offshore wind turbine platforms". *International Journal of Naval Architecture and Ocean Engineering,* ***5***(2), pp. 199–209.

[4] Martin, H. R., 2011. "Development of a scale model wind turbine for testing of offshore floating wind turbine systems". Master's thesis, University of Maine, US.

[5] Li, L., Gao, Y., Hu, Z., Yuan, Z., Day, S., and Li, H., 2018. "Model test research of a semisubmersible floating wind turbine with an improved deficient thrust force correction approach". *Renewable Energy,* ***119***, pp. 95–105.

[6] Nielsen, F. G., Hanson, T. D., and Skaare, B., 2006. "Integrated dynamic analysis of floating offshore wind turbines". In 25th International Conference on Offshore Mechanics and Arctic Engineering, American Society of Mechanical Engineers, pp. 671–679.

[7] Chodnekar, Y. P., Mandal, S., et al., 2015. "Hydrodynamic analysis of floating offshore wind turbine". *Procedia Engineering,* ***116***, pp. 4–11.

[8] de Mello, P., Carneiro, M., Tannuri, E., Kassab, F., Marques, R., Adamowski, J., and Nishimoto, K., 2013. "A control and automation system for wave basins". *Mechatronics,* ***23***(1), pp. 94 – 107.

[9] WAMIT, Inc., 2013. *WAMIT User Manual, Version 7.0*.

[10] Simos, A. N., Ruggeri, F., Watai, R. A., Souto-Iglesias, A., and Lopez-Pavon, C., 2018. "Slow-drift of a floating wind turbine: An assessment of frequency-domain methods based on model tests". *Renewable Energy,* ***116***(4), pp. 133–154.

[11] Venugopal, V., Varyani, K. S., and Barltrop, N. D., 2006. "Wave force coefficients for horizontally submerged rectangular cylinders". *Ocean Engineering*(33), pp. 1669–1704.

[12] Catalano, P., Wang, M., Iaccarino, G., and Moin, P., 33. "Numerical simulation of the flow around a circular cylin-

der at high reynolds numbers". *International Journal of Heat and Fluid Flow*(24), pp. 463–469.

[13] Suzuki, H., Shibata, H., Fujioka, H., Hirabayashi, S., Ishii, K., and Kikuchi, H., 2013. "Development of an analyis code of rotor-floater coupled response of a floating offshore wind turbine". In ASME 32nd Int Conf on Ocean, Offshore and Arctic Engineering (OMAE2013).